Appl. Phys. B 62, 381–387 (1996)

Applied Physics B Lasers and Optics

Dynamic study of gated saturable absorbers

G. Vavra[1], S. Szatmári[1], M. Feuerhake[2]

[1]Department of Experimental Physics, József Attila University, Dóm tér 9, H-6720 Szeged, Hungary
(Fax: + 36-62/311-154)
[2]Laser-Laboratorium Göttingen e.V., D-37016 Göttingen, Germany

Received: 29 May 1995/Accepted: 27 September 1995

Abstract. The capability of gated saturable absorbers for single-pulse selection is studied theoretically using the classical space-time-dependent rate-equation model. The dynamics of operation is followed experimentally by the well-known pump–probe technique. Comparing the theoretical and experimental results, it is found that gated saturable absorbers can efficiently be used for pulse forming and pulse selection of pulses longer than picosecond.

PACS: 42.60

In dye lasers, quenching of the laser action by a strong photon field is known to modulate the output of the laser [1–5]. In the past decades, saturable absorbers (SAs) have been extensively used in many optical experiments. It is shown that the relaxation time of saturable absorbers can be significantly shortened by stimulated emission. Gated saturable absorbers (GSAs) are nonlinear absorbers for which the transmission for a strong input pulse is determined by the combined effect of saturated absorption and stimulated emission of an active medium. The GSA is made of a saturable absorber dye surrounded by a dichroic resonator. The mirrors forming the resonator have high transmission at the wavelength of the input pulses and high reflectivity at the peak wavelength of the emission of the dye.

The idea of this optical arrangement comes from Yasa [6] and further investigations were made in [7, 8]. Experimental realization of pulse shortening by GSAs is reported in [9–11], where the generation of 3–10 ps pulses is demonstrated. Earlier theoretical investigations were only connected to this kind of use of GSAs [12]. It was pointed out that the performance of the GSA used for pulse shortening is critically dependent on the molecular parameters of the dye. When the optimum molecular parameters are chosen, the duration of the transmitted output pulse is found to be proportional to the cavity length and practically independent of the temporal behaviour of the input pulse and of the reflectivity of the resonator mirrors of the GSA.

The time-dependent transmission responsible for pulse shortening makes the GSA potentially suitable for the selection of a single pulse from a pulse train of ultrashort pulses. The feasibility of this idea was also supported by preliminary calculations. However, first experiments to use the GSA for single-pulse selection from a pulse train of femtosecond distributed feedback dye laser (DFDL) pulses were unsuccessful.

The discrepancy between the theoretical and experimental results made it necessary to study the dynamics of the operation of GSAs. The investigations were carried out both theoretically and experimentally, using a rate-equation model and the well-known pump–probe technique, respectively. In this paper, the results of such investigations are presented.

1 Theory

The operation of the GSA is described by the same rate-equation model as used in [12]. The basis of this model is a three-level system ignoring the triplet-state effects and assuming instantaneous vibrational relaxation. The corresponding equations are as follows:

$$\frac{\partial N_1}{\partial t} = \sigma_a N_0(x,t) I_p(x,t) - \sigma_e N_1(x,t)[I_1^+(x,t) + I_1^-(x,t)] - \sigma_a^* N_1(x,t) I_p(x,t) - \frac{N_1(x,t)}{\tau_1} + \frac{N_2(x,t)}{\tau_2},$$

$$\frac{\partial N_2}{\partial t} = \sigma_a^* N_1 I_p(x,t) - \frac{N_2(x,t)}{\tau_2},$$

$$N_0(x,t) + N_1(x,t) + N_2(x,t) = N,$$

$$\pm \frac{\partial I_p^{\pm}}{\partial x} + \frac{n}{c}\frac{\partial I_p^{\pm}}{\partial t} = -\sigma_a N_0(x,t) I_p^{\pm}(x,t) - \sigma_a^* N_1(x,t) I_p^{\pm}(x,y),$$

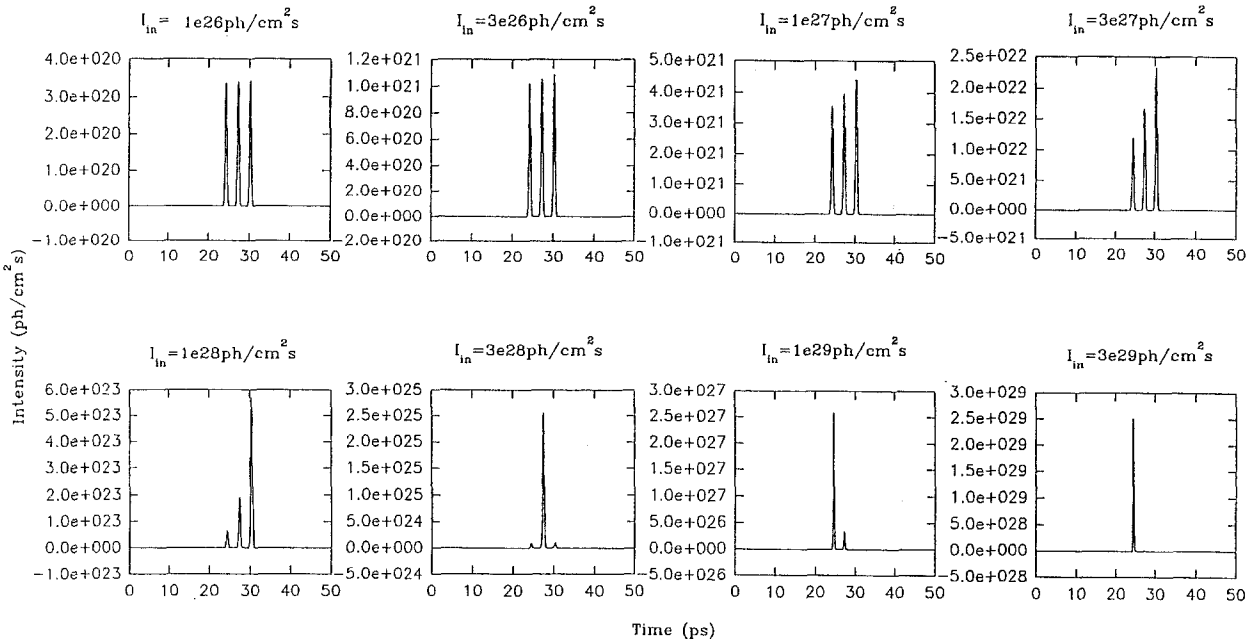

Fig. 1. Response of the GSA on an input pulse train of increasing intensity

$$\pm\frac{\partial I_1^{\pm}}{\partial x}+\frac{n}{c}\frac{\partial I_1^{\pm}}{\partial t}=\sigma_e N_1(x,t)I_1^{\pm}(x,t)+\eta g\frac{N_1(x,t)}{\tau_1},$$

where $I_{p,l}^{\pm}$ is the photon flux at the pumping and lasing wavelength propagating in the $\pm$ direction, respectively,

$$I_p(x,t)=I_p^{+}(x,t)+I_p^{-}(x,t),$$

N is the total density of dye molecules (calculated from a small signal transmission of $T_0=5\times10^{-6}$), N_i is the density of the appropriate singlet state, $i=0,1,2$, σ_a, σ_e, σ_a^* are the cross-sections of absorption, stimulated emission and excited state absorption, respectively, η is the quantum efficiency of the dye (0.71), τ is the fluorescence lifetime of the first and second singlet states, respectively (3.5 ns, 1 ps), n is the index of refraction of dye solution (1.36) and c is the speed of light in vacuum.

The geometrical factor g is calculated as in [7]; $g=0.5[1-2L/(r^2+4L^2)^{1/2}]$, where $r=0.5$ mm is the radius of the homogeneously excited volume, pumped longitudinally by a circular beam.

The multiple trips were treated by the following boundary conditions:

$$I_p^{+}(0,t)=I_{in}(t)+I_p^{-}(0,t)R_p,$$

$$I_p^{-}(L,t)=I_p^{+}(L,t)R_p,$$

$$I_l^{+}(0,t)=I_l^{-}(0,t)R_l,$$

$$I_l^{-}(L,t)=I_l^{+}(L,t)R_l,$$

where R_p, R_l are the reflectivities of the mirrors at the pumping and the lasing wavelength, respectively.

This set of equations was solved numerically by the finite element method. The input was assumed to be a pulse train consisting of three successive uniform Gaussian pulses of 0.5 ps FWHM with a pulse separation of $\tau=3$ ps. These are typical pulses emitted by distributed feedback dye lasers [13]. In the calculations, different parameters have been varied, while the others were kept constant. The initial values of the molecular and cavity parameters were chosen identical to those which were found as optimum in [12] ($\sigma_a=2.0\times10^{-16}$ cm^2, $\sigma_e=2.0\times10^{-16}$ cm^2, $\sigma_a^*=0$ cm^2, $R_p=0.1$, $R_l=0.9$, $L=1$ mm, $T_0=5\times10^{-6}$).

With these parameters, Fig. 1. shows the response of the GSA to an input pulse train consisting of three identical pulses, whose peak intensity is increased from 1×10^{26} ph/cm^2 s to 3×10^{29} ph/cm^2 s. When the input intensity is low, the transmission is comparable to the small signal transmission. Already at low intensities the transmission increases gradually for subsequent pulses due to bleaching the dye. This increase is more pronounced for larger input intensities. If the input laser energy is large enough to initiate laser action in the cavity, it will start cutting the tail of the pulse train, therefore the position of the highest transmission moves from the last pulse to the first one. The normal operation of the GSA occurs at an input intensity of 3×10^{29} ph/cm^2 s (see the last curve of Fig. 1), when the first pulse is already capable of bleaching the GSA and the stimulated emission suppresses all the following pulses. Detailed calculations showed that the operation of the GSA used for pulse suppression depends on the input energy fluence instead of intensity, as long as the input pulse duration is shorter than the lifetime of the excited state. Therefore, in the following the normal operation will be characterized by the input energy fluence.

From the point of view of optimum operation of GSAs–used for single-pulse selection–the right choice of the molecular parameters is found to be fundamental. The critical balance of the saturation of absorption and the stimulated emission can be maintained in a relatively narrow range of parameters. As in the former cases, the

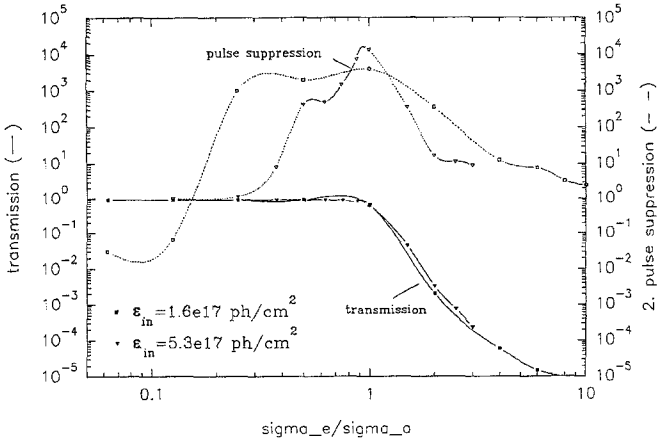

Fig. 2. Dependence of the transmission (*solid line*) and the second pulse suppression (*dashed line*) on the ratio of stimulated emission and absorption cross-section

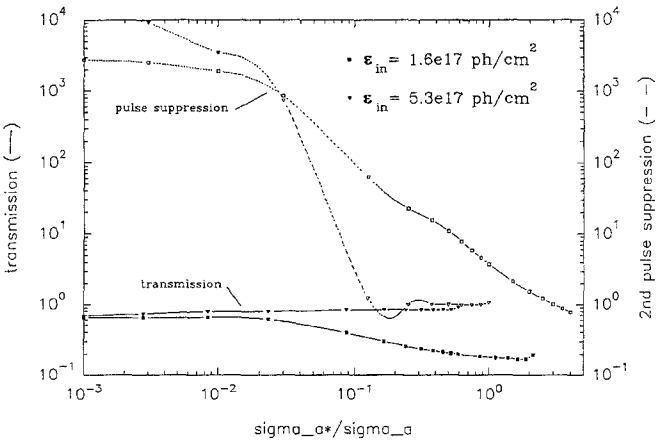

Fig. 3. Dependence of the transmission (*solid line*) and the pulse suppression (*dashed line*) on the ratio of excited-state absorption and absorption cross-section

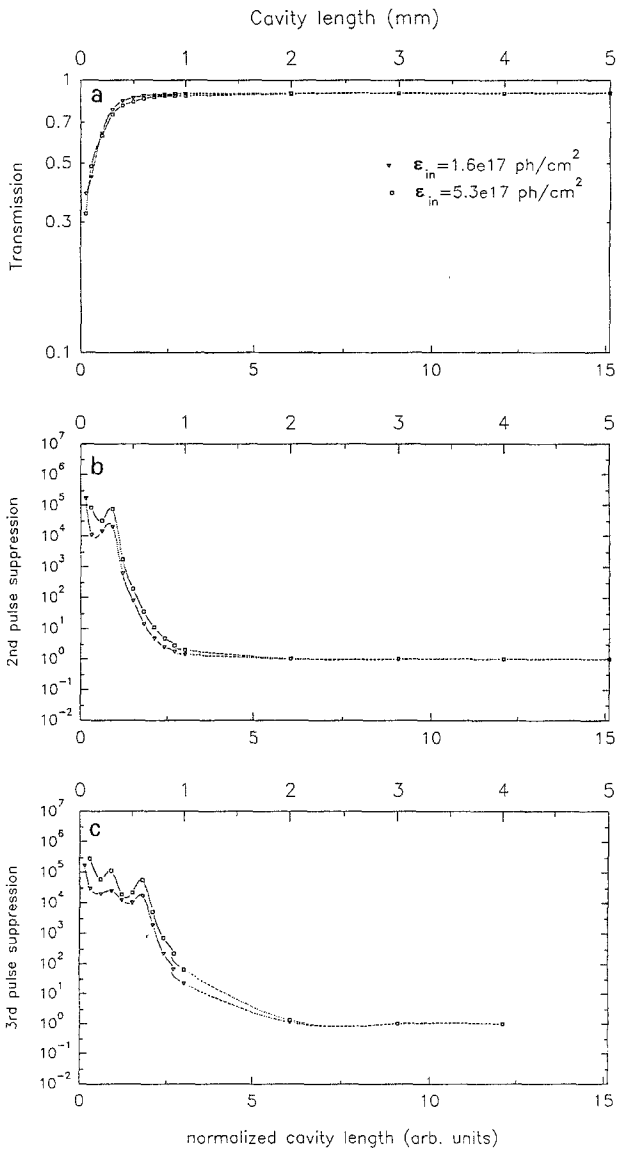

Fig. 4a-c. Dependence of the transmission (**a**), the second (**b**) and the third (**c**) pulse suppression on the cavity length (for the definition of the normalized cavity length, see the text)

ratio of the stimulated emission cross-section at the lasing wavelength (σ_e) to the absorption cross-section for the input pulse (σ_a) has proven to be the most important parameter. In Fig. 2, the transmission for the first pulse and the values of pulse suppression are plotted vs the σ_e/σ_a ratio for input energy fluences corresponding to the normal operation. The transmission is the ratio of the output and input peak intensities of the first pulse, while the pulse suppression factor is defined as the ratio of the peak intensities of the transmitted first and second output pulses. The curves in Fig. 2 are obtained for two input energy fluences. It is seen from the curves that the range of σ_e/σ_a where both the transmission of the first pulse and the pulse suppression factor are optimum is relatively narrow: $0.5 < \sigma_e/\sigma_a < 1.5$. In this range, the dependence of the transmission and pulse suppression on the input energy fluence is relatively weak.

The influence of the excited-state absorption at the pumping wavelength (σ_a^*) of the active medium on the GSA operation is shown in Fig. 3. This influence is not pronounced on the transmission of the first pulse; however the pulse suppression decreases dramatically if the ratio σ_a^*/σ_a exceeds 10^{-2}. As in [12], the stimulated emission at the pumping wavelength (σ_{ep}) is also found to influence the operation; however, here an upper limit of $\sigma_{ep}/\sigma_a \approx 1$ is found.

The other group of parameters, which influences the performance of the GSA, is connected to the cavity of the GSA. Figure 4 shows the dependence of the transmission and pulse suppression on the cavity length of the GSA. The length of the cavity is changed from 0.1 to 5 mm (upper horizontal scale) while the concentration of the active medium is chosen so that the small signal transmission of the GSA is kept constant. A strong decrease of the transmission of the first pulse is obtained when the cavity length is shortened below 0.3 mm. This kind of dependence is caused by the early rise of the stimulated emission in the cavity, which prevents already the transmission of the tail of the first pulse. The earlier the stimulated

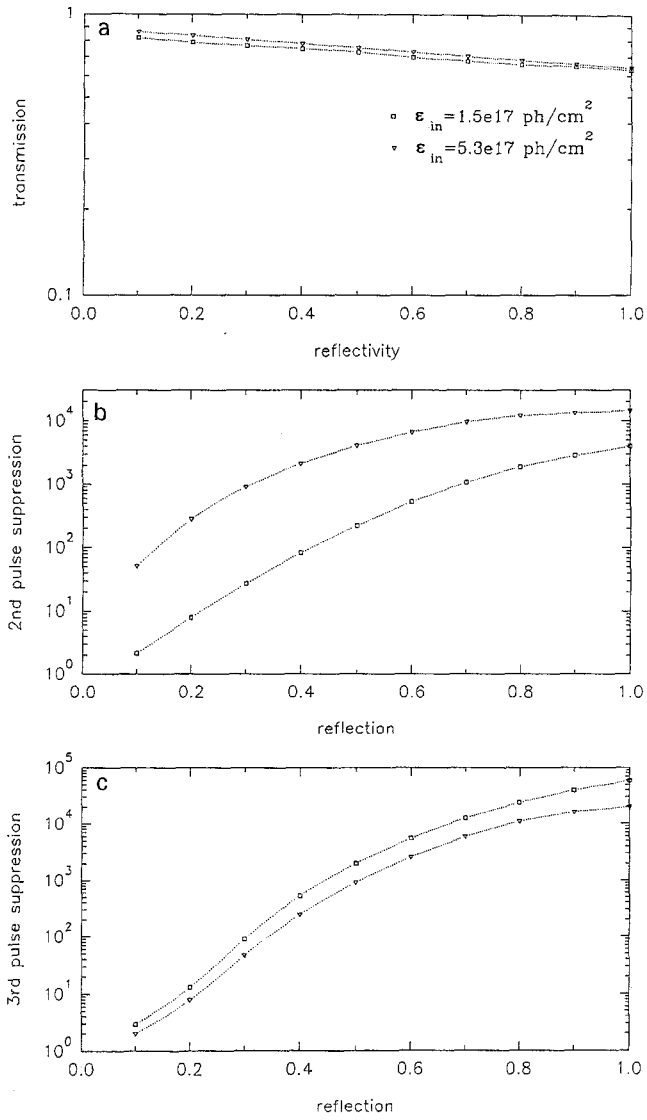

Fig. 5a-c. Dependence of the transmission (**a**), the second (**b**), and the third (**c**) pulse suppression on the reflectivity of the cavity mirrors at the lasing wavelength

emission starts, the more intense the lasing field in the cavity. For this reason, the suppression of subsequent pulses increases. If the stimulated emission starts after the passage of the first pulse (this happens for $L > 0.3$ mm in the calculated case), the initial energy of the lasing field is constant. The intensity of the lasing field at the time of passage of the second incoming pulse decreases with increasing L. This means that the transmission of the first pulse is constant and the suppressions for subsequent pulses decrease for increasing cavity roundtrip time. The pulse suppression is 1 when the roundtrip time is longer than the time separation of the pulses. These dependences can be expressed in a more general way if the transmission and the pulse suppression are referred to as the ratio of the roundtrip time of the resonator ($T = 2nL/c$) and the pulse separation (τ). This "normalized" cavity length is shown as the lower horizontal scale in Fig. 4. According to the calculations and experimental results, the operation of the GSA is only dependent on this normalized cavity length: the same operation is obtained even for input pulses of different pulse separation if the normalized cavity length is chosen constant. The local minima of the pulse suppression curves at certain cavity lengths are explained as spatial effects. These occur when the second pulse propagates together with the lasing pulse generated by the first input pulse along the cavity. In such cases, the lasing field–oscillating between the mirrors–ensures better suppression for the co-propagating second pulse, which decreases the pulse transmission.

The other cavity parameter, whose effect on the suppression was investigated, is the reflection of the mirrors at the lasing wavelengths (R_l). In former investigations, when the GSA was used for pulse forming, a relatively uncritical dependence of the performance of the GSA on R_l was found. However, when the GSA is planned to be used for single-pulse selection (where pumping is not continuous), the "memory-like" feature of the cavity becomes more pronounced, increasing the requirements for R_l. The dependence of the transmission and of the second and third pulse suppression on R_l is shown in Fig. 5a–c, respectively. As expected, the transmission is independent of R_l, while the pulse suppression is decreased if R_l is decreased. Practically acceptable operation is obtained when $R_l \geq 0.7$.

This theoretical model predicts GSAs as being capable of selecting ultrashort pulses from a pulse train, in contrast to former preliminary experiments. According to the calculations, the ratio of the cavity roundtrip time and pulse separation is the determining factor for the operation of the GSA (Fig. 4). For a given cavity length, the time-dependent transmission of the GSA can be studied as the function of the pulse separation of the input pulses using the well-known pump–probe technique. In order to find the origin of the disagreement between theoretical and experimental results, a pump–probe study of the dynamics of the GSA was performed.

2 Experimental

The experiments were performed using a slightly modified Michelson interferometer. The experimental setup is shown in Fig. 6. An input pulse of 10 ps duration, 10 μJ energy at 365 nm was generated by a cascade dye laser system [11]. This pulse was divided by a beamsplitter with a transmission of $T = 65\%$ at 45°. The transmitted part of the input pulse was directed to the GSA using two mirrors, as indicated in Fig. 6. This beam served as a pump

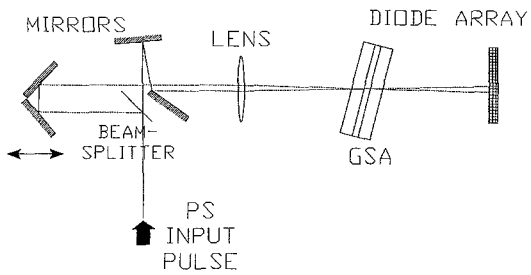

Fig. 6. Experimental arrangement for the pump–probe investigations

pulse. The reflected part of the pulse was sent through a retroreflector made of two aluminium mirrors. The mirrors were built on a movable arm, whose translation was controlled with 1 μm precision. The intensity of this beam was attenuated by neutral filters and served as a probe pulse. The two parallel beams with ~ 0.5 mm diameter and separated by ~ 1 mm were focused by a common quartz lens of $f = 60$ mm focal length onto the active volume of the GSA. The energy influence of the pulses in the GSA could be changed by changing the focusing conditions. Special care was taken to ensure complete spatial overlap between the two beams at the position of the GSA. The optical density of the GSA was always kept unchanged. The plane of the GSA was slightly tilted for easy separation of the transmitted pulses from the stimulated (laser) emission of the GSA. The spatial energy distribution of both pulses was observed by a Hamamatsu 512 pixel linear diode array having a 12.8×0.5 mm^2 sensitive area.

3 Results

The results of the pump–probe measurements for the dynamics of the transmission of the GSA can be studied on the basis of Fig. 7. The x, y, z coordinates represent the delay time between the pump and probe pulses, the linear distribution of both pulses and the energy fluence of the output pulses, respectively. The experimental conditions corresponding to Fig. 7 are the following: the cavity length of the GSA is 1 mm, the dye is 2,5-di-(5-tert-butyl-2-benzoxazolyl)-thiophene (BBOT) of 1×10^{-3} M/l concentration in ethanol. BBOT is chosen as an active medium, since it has been proven both experimentally [10, 11] and theoretically [12] to show satisfactory operation at 365 nm. The fluence of the probe pulse was chosen just to bleach the GSA. The intensity ratio of the pump and probe pulses was set to 3. This choice of the intensity of the pump and probe pulse helped to determine the different aspects of the mechanism. In Fig. 7, the negative time delay corresponds to a situation when the probe pulse arrives earlier than the pump pulse. In this case, the probe is attenuated by the absorption, while for short delays the pump pulse is suppressed by the stimulated emission of the lasing field initiated by the probe pulse. This causes a dip in the pumping intensity. If the delay between the pulses increases, the effect of the weak lasing field caused by the probe pulse decreases, due to the cavity losses. As a result, the intensity of the pump pulse starts to grow. The same happens for positive delays; however, the changes are more pronounced. The stronger lasing field in the GSA induced by the strong pump pulse makes the suppression of the probe pulse much more pronounced. At the time of the arrival of the pump pulse, high transmission of the probe pulse is observed due to the bleaching effect of the pump pulse. The width of this window is in close connection with the cavity length, as shown in [12]: this is the time when the dye has already been bleached, but the stimulated emission has not been developed yet, due to the delay of the cavity. The characteristic features of this time window are seen in Fig. 8a, showing the temporal evolution of the transmission. The slope on the left-hand side is determined by the temporal evolution of the bleaching of the absorber, which in fact is in close connection with the rise-time of the pump pulse [10]. The steeper slope on the right-hand side is the effect of stimulated emission of the lasing field, which is expected to be

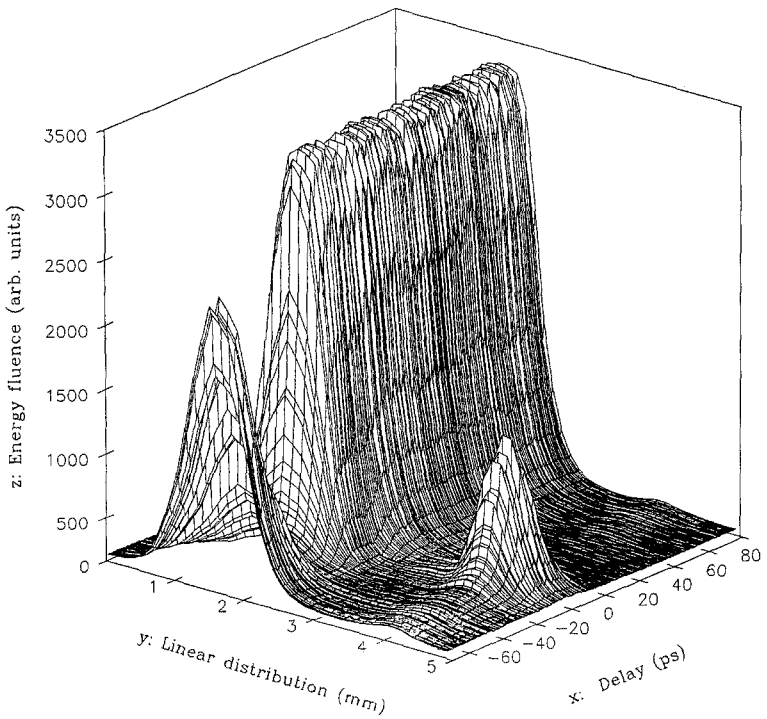

Fig. 7. Typical space-time distribution of the output of the pump–probe experiment

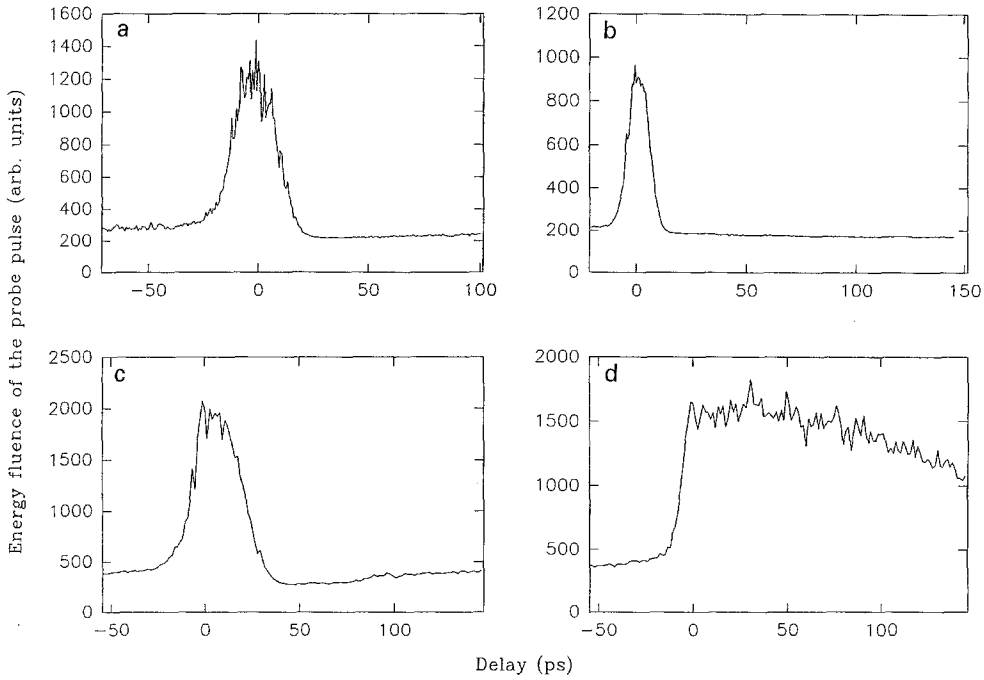

Fig. 8a-d. Temporal behaviour of the transmission for a perfectly aligned GSA of 1 mm (**a**) and 0.5 mm (**b**) cavity length, and for a misaligned GSA of 0.5 mm cavity length with misalignments of $\alpha = 4'$ (**c**), $\alpha = 15'$ (**d**)

always faster than the rise-time of the pump pulse [14]. This asymmetric behaviour is clearly seen in Fig. 8a.

In Fig. 8b, the temporal evolution of the transmission is shown for 0.5 mm cavity length. The intensity of the probe pulse is adjusted so that its effect on bleaching can be neglected. The duration of the bleaching window is about half of the same window in Fig. 8a. The linearity between the cavity length and the duration of the time window (expected from the relevant results of [12]) has been checked for different cavity lengths. In agreement with theoretical calculations, the time window (T) is determined by the cavity length, $T \approx 6nL/c$ [12], as long as the pump pulse duration is comparable to or larger than the cavity roundtrip time ($\tau \geq 2nL/c$). On this basis, one can determine the necessary cavity length for a given pulse train where effective single-pulse selection is excepted.

From the experimental point of view, it is important to know how the operation of the GSA depends on the quality of the cavity. For this reason, the same pump–probe measurements were performed for the same cavity length ($L = 0.5$ mm), but with misaligned cavity mirrors. The results are shown in Fig. 8c–d, where the temporal behaviour of the transmission is shown for increasing misalignments. In Fig. 8c, the transmission curve is shown when the misalignment is $\alpha = 4'$, showing similar performance to Fig. 8b, made with no misalignment. Increasing α, mainly the falling edge of the time window changes; it becomes less steep, resulting in a longer time window. Figure 8d corresponds to such a strong misalignment ($\alpha = 15'$) where the effect of the gated operation is already hardly seen; the absorber remains open after the saturating pump pulse. Similar performance is obtained when the pump–probe study of a standard saturable absorber with no mirrors has been performed.

It is shown by the calculations that the response of the GSA on a pulse train is only determined by the so-called normalized cavity roundtrip time and the pulse separation of the input pulses. This predicts a similar operation for input pulses of different pulse separation and duration if the cavity roundtrip time is correctly chosen. Our experiments show good agreement with the theoretical results (both for pulse shortening and single-pulse selection) when pulses of picosecond duration were used; however, single-pulse selection and pulse forming did not work in former experiments for subpicosecond pulses [10, 11]. Our calculation showed that the "normal operation" of the GSA for given cavity and molecular parameters is achieved when the input pulse has a given energy fluence. For short (subpicosecond) pulses, this energy fluence corresponds to so high intensities where strong self-focusing occurs, preventing the build-up of the photon field in the cavity. This occurs at $\sim 100\,\mathrm{GW/cm^2}$ intensities. Please note that most of the absorbers used in subpicosecond optical experiments are operating in this "nonlinear" regime. However, in those experiments, the good, distortion-free optical cavity is not necessary, since stimulated emission (or lasing) is not required.

The origin of the discrepancy between experiments and theoretical results–beyond the occurrence of possible nonlinearities – can also be related to the instantaneous decay time of vibrational relaxations assumed in our model and to the exclusion of excited-state absorption at the wavelength of lasing. The inclusion of these effects in our model, however, would have made the theoretical treatment much more complicated.

4 Conclusion

The capability of GSAs for single-pulse selection has been studied using a classical space-time-dependent rate-equation model. The dependence of the operation on the cavity, molecular and input parameters is found to be similar to that obtained for GSAs used for pulse shortening. It is found that the single-pulse selection capability is independent of the pulse separation if the so-called normalized cavity length (the ratio of the cavity roundtrip time and pulse separation) is kept constant. However, in practice, efficient single-pulse selection is only obtained for longer than picosecond pulses. This observation is explained by the occurrence of nonlinearities in the case of subpicosecond pulses.

The theoretical and experimental results were supported by pump–probe measurements, which gave an insight into the dynamics of operation of GSAs.

Acknowledgements. The authors wish to thank F.P. Schäfer and G. Marowsky for their continuous interest and stimulating discussions, and P. Simon and Cs. Beleznay for a critical reading of the manuscript. This work has been supported by the OTKA foundation of the Hungarian Academy of Sciences (Contract No. F14303, T14358).

References

1. A. Eranian, P. Dezauzier, O. de Witte: Opt. Commun. **7**, 150 (1973)
2. C. Lin: IEEE J. QE-**11**, 602 (1975)
3. R. Wyett: Appl. Phys. **21**, 353 (1980)
4. F.P. Schäfer, W. Lee, S. Szatmári: Appl. Phys. B **32**, 123 (1983)
5. N.P. Ernsting, B. Nikolaus: Appl. Phys. B **41**, 25 (1986)
6. Z.A. Yasa: J. Appl. Phys. **46**, 4895 (1975)
7. C.G. Christov, I.V. Tomov: Opt. Quantum Electron. **18**, 137 (1986)
8. G.A. Abakumlov, A.I. Antipov, A.P. Simonov, A.B. Sinitsyn, V.V. Fadeev: Sov. J. Quantum Electron. **7**, 1394 (1977)
9. C.G. Christov, I.V. Tomov, I.V. Chaltakov, V.L. Lyutskanov: Opt. Commun. **52**, 211 (1984)
10. S. Szatmári, : Opt. Quantum Electron. **21**, 55 (1989)
11. S. Szatmári, B. Rácz: Opt. Quantum Electron. **18**, 19 (1986)
12. G. Vavra, S. Szatmári: Opt. Quantum Electron. **25**, 733 (1993)
13. S. Szatmári, F.P. Schäfer: Appl. Phys. B **46**, 305 (1988)
14. P.P. Sorokin, K.R. Lankard, E.C. Hammond, V.L. Morizzi: IBM J. Res. Dev. **11**, 130 (1967)